Adsorption (2008) 14: 583–590
DOI 10.1007/s10450-008-9133-x

Hydrogen separation by multi-bed pressure swing adsorption of synthesis gas

Se-Il Yang · Do-Young Choi · Seong-Cheol Jang · Sung-Hyun Kim · Dae-Ki Choi

Received: 1 May 2007 / Revised: 4 November 2007 / Accepted: 18 April 2008 / Published online: 10 May 2008

Abstract The performance of multi-bed pressure swing adsorption (PSA) process for producing high purity hydrogen from synthesis gas was studied experimentally and theoretically using layered beds of activated carbon and zeolite 5A. Nonisothermal and nonadiabatic models, considering linear driving force model and Dual-site Langmuir adsorption isotherm model, were used. The effects of the following PSA variables on separation process were investigated: linear velocity of feed, adsorption time and purge gas quantity. As a result, we recovered a high purity H_2 product (99.999%) with a recovery of 66% from synthesis gas when the pressure was cycled between 1 and 8 atm at ambient temperature.

Keywords Hydrogen separation · Pressure swing adsorption · Synthesis gas

1 Introduction

Hydrogen, regarded as an ecologically clean and renewable energy source, is increasing demanded in various fields including fuel cells, semiconductor processing and petrochemical industry. When the steam reforming technology has been applied to produce hydrogen, it is very important to remove other impurities (mainly CO, CO_2 and CH_4) using adsorption separation technology which is generally considered to be low in energy consumption and very precise in H_2 separation (99.99%) with the aid of pore size and surface characteristics of adsorbent (Ruthven et al. 1994; Yang 1987). Hence, final separation in new hydrogen-producing plants is based on pressure swing adsorption (PSA) utilizing the difference in adsorption properties of various molecules; *e.g.,* components of a gas mixture are selectively adsorbed onto a solid matrix at high pressure and subsequently desorbed by lowering the pressure. A great deal of PSA process concepts have been patented in the last thirty years, several of which have been commercialized (Ruthven 1984).

As hydrogen is separated from synthesis gas using PSA process, layered beds consisting of different adsorbents such as activated carbon and zeolite have been used. Typically carbon dioxide, and a part of methane and carbon monoxide are adsorbed on the first layer of activated carbon while methane and carbon monoxide on the second layer of zeolite (Yang 1987). The performance in the PSA process is usually defined as the purity and recovery of H_2 obtained by executing both experiments and mathematical modelling. The high purity and recovery of the H_2 PSA processes are largely due to an effective operation of multi-bed PSA processes including several pressure equalizations, backfill and layered adsorption bed.

In the present study, hydrogen separation by PSA process using the layered beds of activated carbon (AC) and zeolite 5A (ZL) was investigated experimentally and theoretically to recover high purity H_2 from synthesis gas. All experiments, which were assumed to be non-isothermal and non-adiabatic, were carried out to parametrically analyze the PSA process variables such as linear velocity, adsorption time and purge gas quantity. Aspen Adsim (AspenTech,

S.-I. Yang · D.-Y. Choi (✉) · S.-C. Jang · D.-K. Choi
Division of Environment & Process Technology, Korea Institute of Science and Technology, P.O. BOX 131, Cheongryang, Seoul 130-650, Korea
e-mail: dkchoi@kist.re.kr

S.-H. Kim
Department of Chemical and Biological Engineering, Korea University, Seoul 136-701, Korea

Table 1 Dual-site Langmuir parameters

		k_1 [mmol/g]	k_2 [1/atm]	k_3 [K]	k_4 [mmol/g]	k_5 [1/atm]	k_6 [K]
Activated Carbon	H_2	0.01910	1.90E−05	1170.00	8.73E−04	4.98E−06	1901.46
	CO	0.00423	1.43E−05	2407.68	7.40E−04	2.29E−03	1760.96
	CH_4	0.00576	7.44E−05	2157.02	7.09E−04	2.73E−02	1467.70
	CO_2	0.00764	1.28E−04	2228.63	1.62E−03	2.53E−02	1724.60
Zeolite 5A	H_2	0.00064	1.14E−04	1665.08	3.61E−06	1.96E−16	20848.3
	CO	0.00231	1.17E−04	2652.03	2.54E−03	4.29E−08	3755.31
	CH_4	0.00220	2.08E−04	2298.51	7.31E−04	1.98E−12	7282.80
	CO_2	0.00356	3.01E−03	2923.79	8.23E−04	5.78E−09	5478.58

Inc.) was then utilized for the estimation and the simulation of the PSA process cycles. The simulation results obtained were analyzed numerically by using a non-isothermal dynamic model incorporating mass, energy and momentum balance. By combining the experimental results and the simulation results, we consequently suggest an optimal set of process conditions adequate for maximizing the purity and recovery of the hydrogen product.

2 Mathematical model

An axially dispersed plug flow model was adopted and the linear driving force (LDF) approximation was used. Also, a nonisothermal and nonadiabatic dynamic model was adopted with the following assumptions (Choi et al. 2004; Waldron and Sircar 2000; Ahn et al. 2001):

(1) Ideal gas law applies.
(2) The flow pattern can be described by the axial dispersion plug flow model.
(3) The solid and gas phase reach thermal equilibrium instantaneously.
(4) The mass transfer rate can be represented by a linear driving force (LDF) rate expression.

Based on the above assumptions, the mass balance for each component of the mixture and the total mass balance were written as follows:

Component mass balance:

$$-D_L\frac{\partial^2 C_i}{\partial z^2}+\frac{\partial uC_i}{\partial z}+\frac{\partial C_i}{\partial t}+\frac{1-\varepsilon}{\varepsilon}\rho_p\frac{\partial \bar{q}}{\partial t}=0 \tag{1}$$

Total mass balance:

$$-D_L\frac{\partial^2 C}{\partial z^2}+\frac{\partial uC}{\partial z}+\frac{\partial C}{\partial t}+\frac{1-\varepsilon}{\varepsilon}\rho_p\sum_{i=0}^{n}\frac{\partial \bar{q}_i}{\partial t}=0 \tag{2}$$

Assuming thermal equilibrium between fluid and particles, the energy balance for the gas and solid phase is given by:

$$-K_L\frac{\partial^2 T}{\partial z}+\left(\varepsilon_t\rho_g C_{pg}+\rho_B C_{ps}\right)\frac{\partial T}{\partial t}+\rho_g C_{pg}\varepsilon u\frac{\partial T}{\partial z}-\rho_B\sum_{i}^{n}Q_i\frac{\partial \bar{q}_i}{\partial t}+\frac{2h_i}{R_{B_i}}(T-T_W)=0 \tag{3}$$

Energy balance around the wall of the column is represented as follows:

$$\rho_w C_{pw}A_w\frac{\partial T_w}{\partial t}=2\pi R_B h_i(T-T_w)-2\pi R_{B_o}h_o(T-T_{atm}) \tag{4}$$

Mass transfer rates are expressed as LDF model.

$$\frac{\partial \bar{q}_i}{\partial t}=k_i\left(q_i^*-\bar{q}_i\right) \tag{5}$$

The equilibrium isotherms are assumed to be described by Dual-site Langmuir model (Biegler et al. 2004; Ahn et al. 2006):

$$q_i=\frac{q_{m_i1}B_{i1}Py_i}{1+\sum_k(B_{k1}Py_k)}+\frac{q_{m_i2}B_{i2}Py_i}{1+\sum_k(B_{k2}Py_k)}$$
$$q_{m1}=k_1,\qquad B_1=k_2\exp(k_3/T)$$
$$q_{m2}=k_4,\qquad B_2=k_5\exp(k_6/T) \tag{6}$$

The Dual-site Langmuir parameters are listed in Table 1.

3 Experimental

The adsorbents used in this study were activated carbon (Granular type, 6∼16 mesh) and zeolite 5A (Sphere type, 4∼8 mesh). The activated carbon was supplied by Calgon Corporation with a pellet size of 1.15 mm. The zeolite 5A was supplied by W.R. Grace Corporation with a pellet size of 1.57 mm. The physical properties of the adsorbents and

Table 2 Physical properties of adsorbents and bed

Adsorbents			
		Activated Carbon	Zeolite 5A
Average pellet size	(mm)	1.15	1.57
Pellet density	(g/cm^3)	0.85	1.16
Bulk density	(g/cm^3)	0.482	0.764
Heat capacity	(cal/g·K)	0.25	0.21
Bed			
Length	(cm)	55	25
Inside diameter	(cm)		2.7
Outside diameter	(cm)		3.5
Heat capacity of column	(cal/g·K)		0.12
Density of column	(g/cm^3)		7.83
Internal heat transfer coefficient	(kJ/s·m^3·K)		0.0385
External heat transfer coefficient	(kJ/s·m^3·K)		0.0142
Bulk density	(g/cm^3)	0.532	0.744
External void fraction	(–)	0.433	0.357

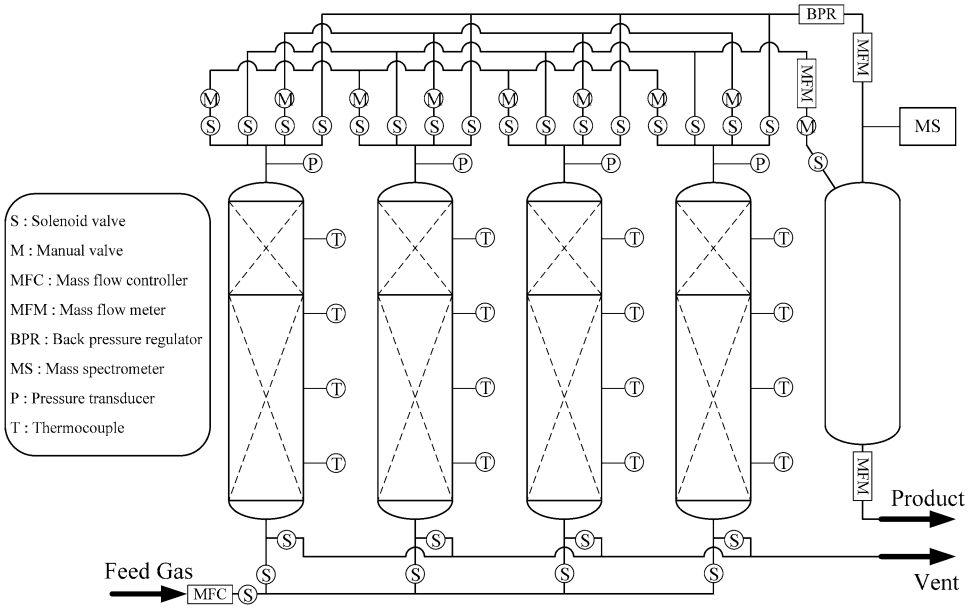

Fig. 1 Four-bed PSA process

bed listed in Table 2. Based on steam methane reforming off gas composition, the gas mixture of composition, H_2: 72.2%, CO_2: 21.6%, CO: 2.03%, CH_4: 4.17%, were used.

A schematic diagram of the apparatus used is presented in Fig. 1. The four columns were fabricated from the stainless steel pipe of 2.7 cm ID, 80 cm length, and 0.39 cm wall thickness and packed with activated carbon and zeolite 5A adsorbents. The activated carbon layer height is 55 cm at the feed end and the zeolite 5A layer height is 25 cm above activated carbon layer. The four thermocouples (K type) were installed at each of four columns and located in the bed of 10, 30, 50, and 70 cm distant from the top of the packed section, at the center and at half the bed radius in order to track the thermal wave front. The pressure transducers were installed at the top of each column in order to measure the pressure profile. A product storage vessel was installed at the product end from which the product backfill gas was supplied. The flowrates of feed, purge and product were controlled and measured using mass flow controller and mass flow meter. The adsorption pressure was controlled by back pressure regulator. The rates of pressurization, purge, and pressure equalization were controlled by hand control valve. The sampling port was placed downstream of the mass flow meter, so that the product flow rate could be measured without any loss due to sampling. The product concentrations are monitored continuously and automatically with a mass spec-

Table 3 Operating conditions in experimental runs

Run	P^F [atm]	P^4 [atm]	v_f* [cm/s]	t_c [sec]	t_{AD} [sec]	ΔP** [atm]
A	8	1	2.5	200	50	2.0
B	8	1	3.0	200	50	2.0
C	8	1	3.5	200	50	2.0
D	8	1	3.0	160	40	2.0
E	8	1	3.0	240	60	2.0
F	8	1	3.0	200	50	1.2
G	8	1	3.0	200	50	2.8

*Linear velocity

**Difference between pressures before and after provide purge step

trometer (Omnistar 300). The control of the solenoid valve switching and the data acquisition of measuring variables were done by a PLC (National Instruments) linked to a personal computer whose monitor provided an on-line display of dynamic changes in all measured values.

The experimental operation conditions are summarized in Table 3. In these cycles, the purge gas quantity is determined by the pressure difference (ΔP) during the Provide Purge (PP) step. The larger ΔP, the more quantity is used in the purge. In every experimental run, the duration of adsorption pressure was set to 8 atm. The adsorption time varied from 40 to 60 s. The change of the linear velocity, the adsorption time and the purge gas quantity were studied.

4 Cycles of the 4-bed 9-step PSA process

The PSA process designed on the basis of Batta cycles for this study consisted of the following nine cycle steps (Waldron and Sircar 2000; Sircar and Golden 2000; Batta 1971; Doong and Yang 1987):

(a) Adsorption (AD): Feed gas is passed at pressure P^F through an adsorber and pure H_2 stream is produced through the product end at the feed gas pressure. This step was continued until the impurity front reached about the middle of the column.
(b) First Pressure Equalization I (EQI-BD): The adsorber is then cocurrently depressurized to a pressure level of P^1. Pure H_2 is produced through the product end which is utilized to partially pressurize another column undergoing step (h).
(c) Provide Purge (PP): The column is then concurrently depressurized to a pressure level of P^2. The effluent gas in this step is used to purge another column undergoing step (f).
(d) Second Pressure Equalization (EQII-BD): The column is further depressurized cocurrently to a pressure level of P^3. The effluent gas through the product end, that is, a high purity H_2 is used to pressurize another column undergoing step (g).
(e) Blow down (BD): The column is then countercurrently depressurized to the lowest pressure level of cycle (P^4). The effluent gas, which contains a part of the desorbed gases and most of the column void gases, is wasted.
(f) Purge (PG): The column is then countercurrently purged with pure H_2 at pressure P^4 obtained from a column undergoing step (c). The effluent gas in this step contains the remains of the desorbed impurities, which is then wasted.
(g) Second Pressure Equalization (EQII-PR): The column is then pressurized from pressure P^4 to P^5 by countercurrently introducing the gas produced by a column undergoing step (d).
(h) First Pressure Equalization (EQI-PR): The column is further pressurized from P^5 to P^6 by countercurrently introducing the effluent gas from step (b).
(i) Backfill (BF): Finally, The column pressure was raised from P^6 to PF by introducing a part of the H_2 product gas from product tank. The adsorber is now ready for the next cycle from step (a) to step (i).

Figure 2 shows the pressure history for the above-mentioned PSA process and Table 4 presents the cycle steps and time schedules. The pressure histories in all experiments and simulations were observed to be identical. The impurities were adsorbed from the feed gas in step (a), which were afterwards desorbed and removed from the column in steps (e) and (f). The steps (b) and (d) are added to recover and internally recycle a part of the void and co-adsorbed H_2 in the end of the column. The step (c) also recovers a part of the void and co-adsorbed H_2, and recovery H_2 gas at this step is used as the purge gas of another column. The impurities are not allowed to break through the product end of the column until the end of the second pressure equalization step (d). The effluent waste gases were produced during steps (e) and (f).

5 Results and discussion

5.1 Effect of linear velocity

The linear velocity is one of key parameters in determining the productivity of the PSA process. As the linear velocity increased, the productivity increased but the product purity decreased. Figure 3 shows the process performance obtained with different linear velocities at adsorption pressure of 8 atm and adsorption time of 50 s. Figure 4 shows concentration profiles of CH_4, CO and CO_2 in gas phase at the end of second pressure equalization step with the linear velocity of 2.5, 3.0 and 3.5 cm/s. When the linear velocity

Table 4 Cycle steps for the PSA process

Cycle times (s)	$t_c/4$			$t_c/24$	$t_c/6$	$t_c/24$	$t_c/24$	$t_c/6$	$t_c/24$	$t_c/24$	$5t_c/24$	
Bed A	AD			EQI-BD	PP	EQII-BD	BD	PU	EQII-PR	EQI-PR	BF	
Bed B	EQI-PR	BF		AD			EQI-BD	PP	EQII-BD	BD	PU	EQII-PR
Bed C	BD	PU	EQII-PR	EQI-PR	BF		AD			EQI-BD	PP	EQII-BD
Bed D	EQI-BD	PP	EQII-BD	BD	PU	EQII-PR	EQI-PR	BF		AD		

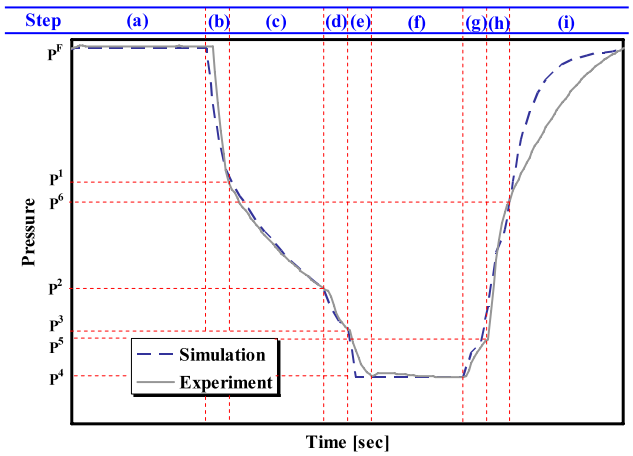

Fig. 2 Pressure history

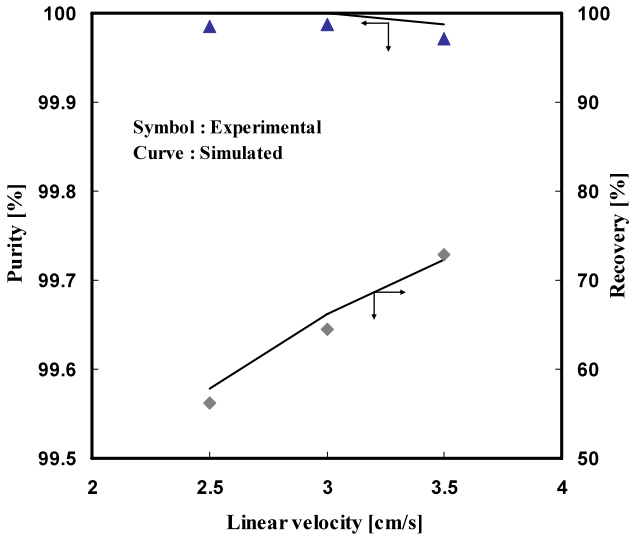

Fig. 3 PSA process performance using different linear velocities of feed

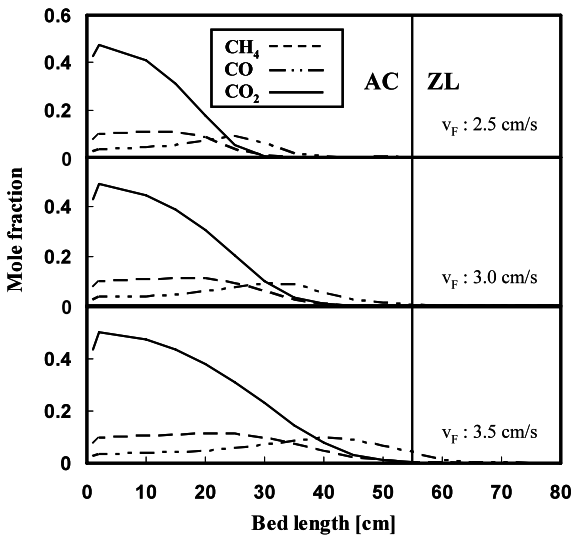

Fig. 4 Concentration profile in gas phase at the end of second pressure equalization step

increased from 2.5 to 3.0 cm/s, the purity was similar above 99.999% but the recovery increased from 58 to 66%. This result means that the CO in gas phase at the end of last pressure equalization step reaches about the middle of the adsorber at the linear velocity of 2.5 cm/s, indicating that such a linear velocity is not high enough to use packing adsorbent in adsorber. With further increasing the linear velocity to 3.5 cm/s, the recovery increased from 66 to 72% while the purity decreased from 99.999 to 99.987% since the CO and CH_4 in gas phase at the end of last pressure equalization step are exhausted at the end of the column, which is due to the increase in the length of the mass transfer zone. Therefore, the linear velocity of 3.0 cm/s, with which the impurities are not exhausted at the end of the column until last pressure equalization step, is determined in this study.

5.2 Effect of adsorption time

In a PSA process the total cycle time is determined by the adsorption time related to the breakthrough which occurs when the impurities reach the end of the column. Jain et al. (2003) decided the adsorption time near the breakthrough time for the purpose of obtaining the purity 99% in a 2-bed PSA process. However in case of a 4-bed 9-step PSA process, the product purity declines when the adsorption time is decided near the breakthrough time in a 4-bed 9-step PSA process, due to complicated cycle steps. Also, the adsorption time should be shorter than the breakthrough time so that high hydrogen purity 99.999% is attainable. So far, we determined the adsorption time (about 50 s) near one-fifth of breakthrough time.

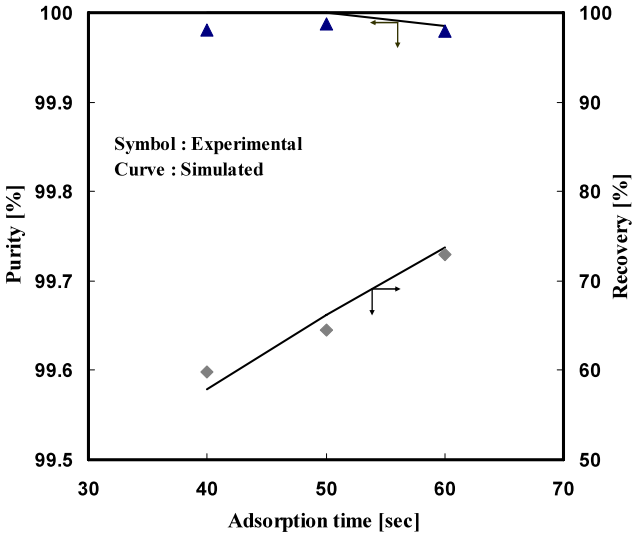

Fig. 5 PSA process performance using different adsorption time (t_{AD})

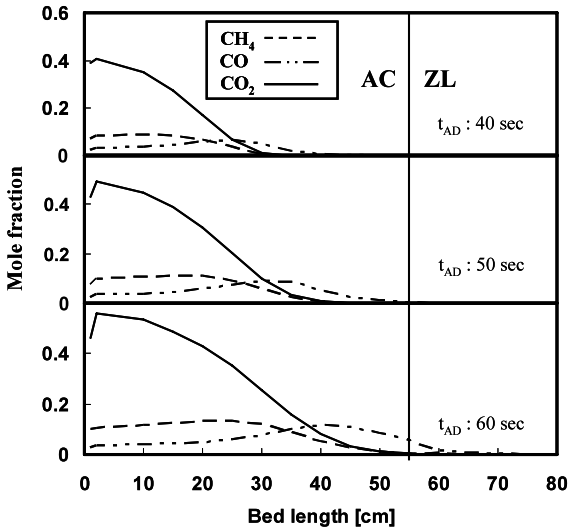

Fig. 6 Concentration profiles in gas phase at the end of second pressure equalization step

Figure 5 shows the process performance obtained with different adsorption times at adsorption pressure of 8 atm and linear velocity of 3.0 cm/s. The product recovery (58%) with the adsorption time of 40 s was lower than that (66%) with the adsorption time of 50 s whereas the purity (> 99.999%) was observed similarly with both adsorption times. This decrease in the product recovery results from a large amount of hydrogen remaining in the bed until the last pressure equalization step. On the other hand, the purity and recovery were 99.985% and 73%, respectively, with the adsorption time of 60 s. Such a longer adsorption time will render productivity high and the rate of the increase of product recovery much greater than that of the decrease of product purity. Figure 6 shows the concentration profiles in gas phase at the end of second pressure equalization step with different adsorption times. As the adsorption time increased from 40 to 60 s, mass transfer zone of impurities approached toward the end of the column. Especially, as the adsorption time increased from 50 to 60 s, the impurities, CO and CH_4, break through the product end of the column until the end of the last pressure equalization step. Therefore, the PSA process with the adsorption time of 50 s was operated in this study.

5.3 Effect of purge gas quantity

The purge gas quantity can be defined as the pressure difference (ΔP) between the pressure at the end of the first pressure equalization step and that at the end of the provide purge step which delivers purge gas to the low pressure column. Such a pressure difference strongly affects the recovery and purity of the product; *i.e.*, as ΔP becomes smaller, more hydrogen product can be recovered with decreasing its purity but, as ΔP is larger, purging becomes more effective,

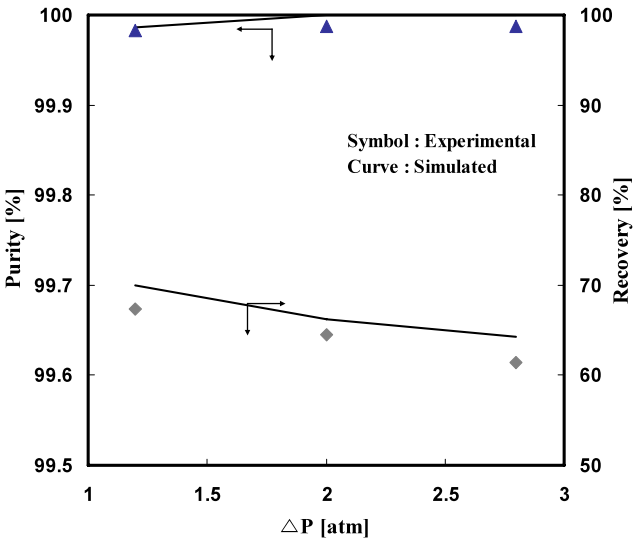

Fig. 7 PSA process performance using different purge gas quantity

providing a regenerated bed with less adsorbents and an increased hydrogen purity. Figure 7 shows the process performance obtained with different ΔP's at adsorption pressure of 8 atm, linear velocity of 3 cm/s and adsorption time of 50 s. When ΔP was larger than 2.0 atm, the purity did not change much but the recovery continuously decreased from 66 to 64% with increasing ΔP. However, the hydrogen purity decreased from 99.999 to 99.987% with decreasing ΔP from 2.0 to 1.2 atm. The reason leading to this result can be interpreted in two respects; *i.e.*, one is that the impurities are exhausted at the end of the column with result of its accumulation in the column, and the other is that gases of lower hydrogen purities are used in the provide purge step and pressure equalization steps (Doong and Yang 1987). Figure 8

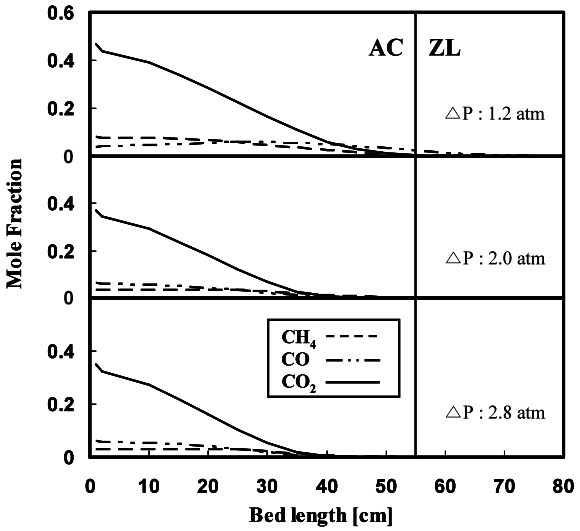

Fig. 8 Concentration profile in gas phase at the end of provide purge step

shows the concentration profiles in gas phase at the end of provide purge step with different ΔP's. The CO is not desorbed well from zeolite 5A layer at ΔP of 1.2 atm because of small purge gas quantity. Also, as ΔP increased from 1.2 to 2.8 atm, the impurities are descended downward to the bottom in the column. On the basis of these results, we can infer that ΔP should be neither too low nor too high, suggesting that the PSA process in this study should be operated around ΔP of 2 atm.

6 Conclusions

Using a layered bed of activated carbon and zeolite 5A, a 4-bed 9-step PSA process was studied theoretically and experimentally to produce a high purity H_2 product from synthesis gas. The effects of the linear velocity of feed, the adsorption time, and purge gas quantity on the process performance were investigated. The nonisothermal, bulk separation PSA model adopted the linear driving force approximation for the particle uptake and the adsorption isotherm used the Dual-site Langmuir. All the experimental results were in good agreement with the values predicted by the theoretical model.

High purity H_2 product (99.999%) can be produced at feed gas pressure (8 atm) from synthesis gas (H_2: 72.2%, CH_4: 4.17%, CO: 2.03%, CO_2: 21.6%). The H_2 recovery increased with increasing the linear velocity and adsorption time, but the H_2 purity was on the reverse. Therefore, the linear velocity and the adsorption time can increase until the impurities reach the product end of the column until second pressure equalization step. At a given H_2 purity, H_2 recovery and the productivity increased with decreasing ΔP at provide purge step. In this study, the 4-bed 9-step PSA process could be optimally operated at the linear velocity of 3 cm/s, adsorption time of 50 s and ΔP of 2 atm at the provide purge step, finally leading to, at least, more than 66% H_2 recovery.

Notation

A_w	cross sectional area, cm^2
C	concentration of adsorbate, mol/g
C_{pg}	gas heat capacity, cal/g/K
C_{ps}	particle heat capacity, cal/g/K
C_{pw}	column wall heat capacity, cal/g/K
D_L	Knudsen diffusivity, cm^2/s
h	heat transfer coefficient, $cal/cm^2 \cdot s \cdot K$
k	linear driving force mass transfer coefficient, s^{-1}
k_{1-6}	dual-site Langmuir isotherm model parameter
K_L	effective axial thermal conductivity, $cal/cm^2 \cdot s \cdot K$
P	pressure, atm
q	equilibrium mole adsorbed, mol/g
q^*	equilibrium adsorbed phase concentration, mol/g
Q	average isosteric heat of adsorption, cal/mol
R	gas constant, cal/mol·K
R_B	bed radius, cm
t	time, s
T	temperature, K
T_{atm}	ambient temperature, K
T_w	wall temperature, K
u	interstitial velocity, cm/s
V	volume, cm^3
y	mole fraction in gas phase
z	axial position in a adsorption column, cm

Greek Letters

ε	interparticle void fraction
ε_t	total void fraction
ρ_B	bulk density, cm^3/g
ρ_g	gas density, cm^3/g
ρ_p	particle density, cm^3/g
ρ_w	column density, cm^3/g

Acknowledgement This work was supported by SK Corporation and National RDND Organization for Hydrogen & Fuel Cell, Ministry of Commerce Industry and Energy.

References

Ahn, H.W., Yang, J.Y., Lee, C.H.: Effects of feed composition of coke oven gas on a layered bed H_2 PSA process. Adsorption **7**, 339–356 (2001)

Ahn, E.S., Jang, S.E., Choi, D.Y., Kim, S.H., Choi, D.K.: Pure gas adsorption equilibrium for $H_2/CO/CO_2$ and their binary mixture on zeolite 5A. Korean Chem. Eng. Res. **44**, 460–467 (2006)

Batta, L.B.: Selective adsorption process. US patent 3,564,816 (1971)

Biegler, L.T., Jiang, L., Fox, V.G.: Recent advances in simulation and optimal design of pressure swing adsorption systems. Sep. Purif. Rev. **33**, 1–39 (2004)

Choi, B.U., Nam, G.M., Choi, D.K., Lee, B.K., Kim, S.H., Lee, C.H.: Adsorption and regeneration dynamic characteristics of methane and hydrogen binary system. Korean J. Chem. Eng. **21**, 821–828 (2004)

Doong, S.J., Yang, R.T.: Hydrogen purification by the multi-bed pressure swing adsorption process. React. Polym. **6**, 7–13 (1987)

Jain, S., Moharir, A.S., Li, P., Wozny, G.: Heuristic design of pressure swing adsorption: a preliminary study. Sep. Purif. Technol. **33**, 25–43 (2003)

Ruthven, D.M.: Principles of Adsorption and Adsorption Processes. Wiley, New York (1984)

Ruthven, D.M., Farooq, S., Knaebel, K.S.: Pressure Swing Adsorption. VCH, New York (1994)

Sircar, S., Golden, T.C.: Purification of hydrogen by pressure swing adsorption. Sep. Sci. Technol. **35**, 667–687 (2000)

Waldron, W.E., Sircar, S.: Parametric study of a pressure swing adsorption process. Adsorption **6**, 179–188 (2000)

Yang, R.T.: Gas Separation by Adsorption Process. Butterworth, Boston (1987)